environments

*Article*

# Soil Organic Carbon Depletion in Managed Temperate Forests: Two Case Studies from the Apennine Chain in the Emilia-Romagna Region (Northern Italy)

**Valentina Brombin [1], Gian Marco Salani [1,2], Mauro De Feudis [3], Enrico Mistri [1], Nicola Precisvalle [1] and Gianluca Bianchini [1,*]**

[1] Department of Physics and Earth Sciences, University of Ferrara, 44122 Ferrara, Italy; brmvnt@unife.it (V.B.); slngmr@unife.it (G.M.S.); enrico.mistri@unife.it (E.M.); prcncl@unife.it (N.P.)
[2] Department of Chemical, Pharmaceutical and Agricultural Sciences, University of Ferrara, 44122 Ferrara, Italy
[3] Department of Agricultural and Food Sciences, Alma Mater Studiorum, University of Bologna, 40127 Bologna, Italy; mauro.defeudis2@unibo.it
* Correspondence: bncglc@unife.it

**Abstract:** Forest soils contain a large amount of organic carbon (OC); therefore, small changes in these ecosystems have effects on climate. In this study, variation in the quantity of C pools that occurred in one year in the soil of temperate forests managed by two farms in the Apennine chain (Emilia-Romagna Region) was investigated using elemental and isotopic C analyses of soil samples collected in 2020 and 2021. In one year, soil from the Branchicciolo (BRA) farm lost organic matter as shown by the decrease in C contents and the less negative C isotopic signatures ($^{13}C/^{12}C$), whereas the C contents and C isotopic signatures remained almost stable during time in the soil from the Beghelli (BEG) farm. This cannot be related to thinning interventions, as much more forest material was removed from the BEG forest than from the BRA forest (60% and 25%, respectively). Therefore, other causes should be considered. The BRA forest was at a lower altitude than the BEG forest; thus, it was more affected by C depletion due to the warmer temperature. Moreover, the sandy soil in the BRA forest was less prone to sequestering organic matter than the soil in the BEG forest, which was characterized by phyllosilicates (including vermiculite) and zeolites (clinoptinolite) having high C sequestration capacity. This work showed the different impacts of the pedo-climatic conditions in two nearby farms, which should be considered in planning appropriate silvicultural management for OC sequestration.

**Keywords:** soil; forest; carbon; isotopic signature; climate change; silvicultural management



**Citation:** Brombin, V.; Salani, G.M.; De Feudis, M.; Mistri, E.; Precisvalle, N.; Bianchini, G. Soil Organic Carbon Depletion in Managed Temperate Forests: Two Case Studies from the Apennine Chain in the Emilia-Romagna Region (Northern Italy). *Environments* **2023**, *10*, 156. https://doi.org/10.3390/environments10090156

Academic Editor: Joaquim Esteves Da Silva

Received: 5 August 2023
Revised: 5 September 2023
Accepted: 7 September 2023
Published: 9 September 2023



## 1. Introduction

Soil is the central interface of Earth's critical zone, i.e., the layer of our planet where the lithosphere, hydrosphere, atmosphere, biosphere, and, recently, anthroposphere interact with each other; thus, it is most vulnerable to the effects of climate and/or anthropic activities [1]. Soil is also one of the most important ecosystem resources; however, it is not renewable on the human generation scale [2]. Its ecological functions are numerous and include nutrient cycling, water regulation, filtering, supporting plant systems and human structures, promoting biodiversity and habitat, and carbon storage and turnover [3,4]. Soils store carbon (C) in an inorganic form (SIC), which is derived from carbonatic minerals, and an organic form (SOC), which is derived from the decomposition of soil organic matter (SOM) [5]. Globally, soils store 2500 gigatons (Gt) of C, including 1550 Gt of SOC and 950 Gt of SIC. The amount of C in the soil is ~3 and ~4.5 times more than the atmosphere pool (760 Gt) and the biosphere pool (560 Gt), respectively [6–9]. More than 40% (860 Gt) of the OC in terrestrial ecosystems is stored in forest soils [10,11], which means that forests play a major role in the C cycle, second only to the oceans [12]. Pan and

Birdsey [10] and Köhl and Lasco [13] calculated that world forest ecosystems remove nearly 2 Gt year$^{-1}$ of C from the atmosphere, thereby absorbing about 30% of anthropogenic $CO_2$ emissions. However, climate change is exerting substantial effects on forest ecosystems worldwide, posing risks to the ability of forests to sequester C [14–16]. In the current climate change model, sustainable forest management practices and the related C sequestration are becoming a priority for our society. Therefore, several works investigated the impact of different silvicultural practices on C sequestration, such as afforestation, harvesting, thinning, fertilization, and drainage of peatlands and wetlands (see for a review [17]). However, a deep understanding of the SOM processes and related factors is still required to reconstruct C cycle dynamics in the forest ecosystem [17]. In this context, the Rural Development Program (RDP) of the Emilia-Romagna Region (Northern Italy) financed the SuoBo project, which aims to assess and preserve the quantity and quality of SOM in two mountainous forest ecosystems located on the Apennine chain of the Emilia-Romagna Region. To reach such general aims of the project, the present study deals with investigating the soil C forms and their relationships with the pedo-climatic conditions taking into consideration two forest ecosystems. The two selected farms were located close to each other (15 km), but they were at different altitudes, and the soils were characterized by different textures. For this work soil samples were collected from both farms in 2020 and 2021 in the same locations to assess any variations in soil OC pools occurring in one year at both farms and explore the possible natural (e.g., pedo-climatic conditions) and/or anthropic (e.g., silvicultural practices) causes. In detail, both the total C and the OC fractions were measured and isotopically characterized in two soil layers (0–15 and 15–30 cm; top- and subsoil, respectively) at the farms, to assess any increase or decrease in C and the modifications to the isotopic signature, as Teng and Ma [18] pointed out the importance of deciphering the isotopic signature of the Earth's surface and critical zone processes. In addition, this project quantified the OC pools, characterized by different turnover and permanence in the soil (e.g., labile and stabile pools). This comprehensive approach allowed us to evaluate SOM evolution and thus assess C sequestration and/or GHG release from the mountainous forest soils.

## 2. Materials and Methods

### *2.1. Sites Description*

Two temperate forests were selected along the Northern Apennines in the Emilia-Romagna region (Northern Italy; Figure 1a). One study site was an uneven-aged deciduous forest of oak, hornbeam, and walnut trees located at Sasso Marconi (44°20′15″N, 11°16′32″E) at about 225 m above sea level (a.s.l.) and exposed at southwest. This was managed by the "Branchicciolo farm" (BRA; Figure 1b). The BRA forest was situated on deposits formed after multiple landslides in the surrounding mountains, where a limestone–sandstone sedimentary succession crops out (Figure 1b). The other study site was an uneven-aged chestnut forest located in Monte San Pietro (44°24′19″N, 11°07′24″E) at about 560 m a.s.l. and located on a north-facing slope. This was managed by the "Beghelli farm" (BEG; Figure 1c). The BEG forest was located on a silty succession (Figure 1c). The forests were 15 km apart (Figure 1a), and both had a humid subtropical climate with hot, humid summers (June–August) and cold, humid winters (December–February). However, due to the different altitudes, the two areas experienced different mean temperatures and precipitation. In 2020, at Sasso Marconi, the mean annual temperature was 14.2 °C, and the average annual rainfall was 671 mm, whereas at Monte San Pietro, the mean annual temperature was 13.8 °C, and the average rainfall was 723 mm [19]. In 2021, at Sasso Marconi, the mean annual temperature was 15 °C, and the average annual rainfall was 509 mm, whereas, at Monte San Pietro, the mean annual temperature and rainfall were 14.3 °C and 520 mm, respectively [20].

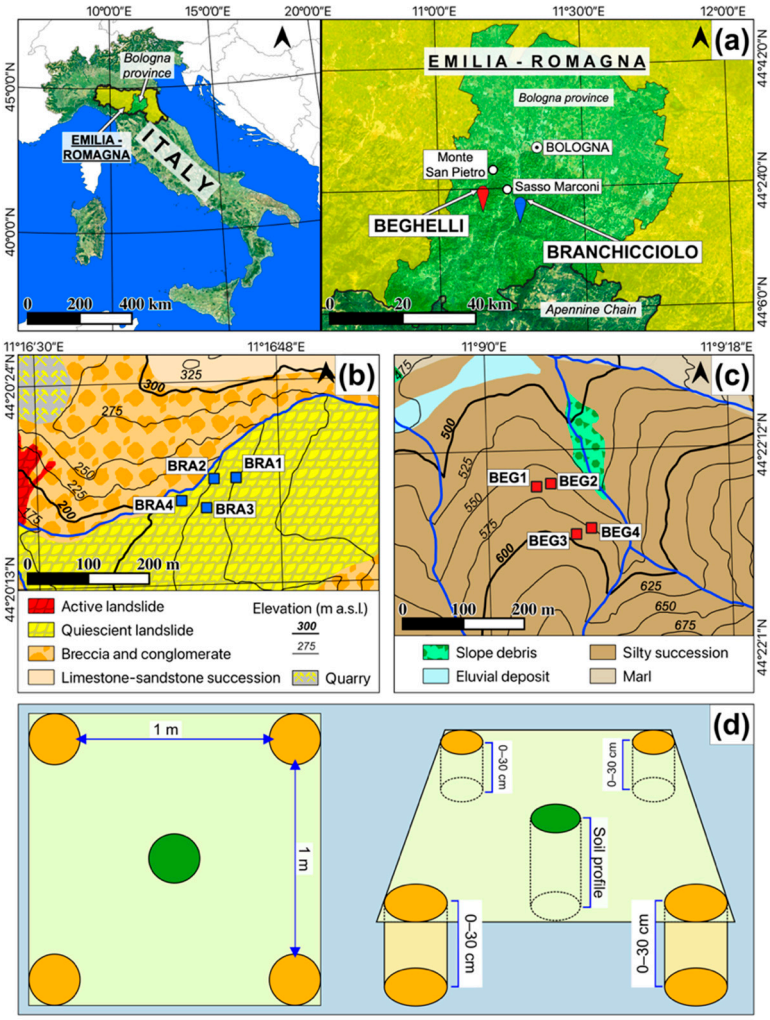


**Figure 1.** (**a**) Locations of the investigated farms in the Apennine chain of the Emilia-Romagna Region (Northern Italy). Simplified geomorphological maps of the studied areas showing the location of (**b**) the mixed forest at the Branchicciolo (BRA) farm and (**c**) the chestnut forest at the Beghelli (BEG) farm. (**d**) Schematic design showing the sampling: At each farm, four sites were identified; at the center of each plot, a soil profile and four 0–30 cm depth pits were dug. For each site, soil layers at 0–15 cm and 15–30 cm depth were collected from each minipit and deciduous to obtain a composite sample.

### *2.2. Sampling*

In both forests, the first soil sampling was performed in October 2020, and the second sampling was performed one year later: in July 2021 at BRA and in September 2021 at BEG. After the soil sampling carried out in 2020, within the study sites, a thinning treatment was performed with the removal of 25% of the stems (mainly dead and unhealthy plants) at the BRA forest and with the removal of 60% of the forest material (i.e., stems, understory bushes, poor-quality trees) at the BEG forest. All remaining harvested trees and all plant residues were removed from the sites.

To perform the sampling, in each area, four sites were identified at different slopes (Table 1).

In each study site, four soil profiles were dug down to the pedological substrate in 2020. For each soil profile, genetic horizons were described and sampled as indicated by Schoeneberger et al. [21]. In addition, a fixed-depth sampling (0–15 and 15–30 cm) was performed in each site in 2020 and 2021 (Figure 2). In particular, close to each soil profile, four pits were dug down to 30 cm depth (starting from the A horizon), and the samples

were collected from the 0–15 and 15–30 cm intervals. The samples from the same interval depth were merged to obtain a composite sample.

**Table 1.** The slope of sites identified in the Branchicciolo (BRA) forest and the Beghelli (BEG) forest.

| Site | Slope (%) |
|---|---|
| Branchicciolo forest | |
| BRA1 | 20 |
| BRA2 | 5 |
| BRA3 | 3 |
| BRA4 | 45 |
| Beghelli forest | |
| BEG1 | 20 |
| BEG2 | 45 |
| BEG3 | 32 |
| BEG4 | 45 |


**Figure 2.** Sampling soil layers (0–15 cm and 15–30 cm) from a minipit dug at one of the farms investigated by the SuoBo project.

### *2.3. Soil Sample Preparation, Textural Analysis, and Determination of Physicochemical Parameters*

The composite soil samples were air-dried and sieved at 2 mm. For the <2 mm soil fractions, the particle size distribution was investigated using the pipette method, after dispersion of the sample with a sodium hexametaphosphate solution [22]. The pH value was determined potentiometrically in a 1:2.5 (*w*/*v*) soil:distilled water suspension with a Crison pH meter. The electrical conductivity (EC) was also performed in a 1:2.5 (*w*/*v*) soil:distilled water suspension with an Orion conductivity meter. Additionally, an aliquot of the <2 mm sample was powdered in an agate mill. In the powdered samples, the carbonate content was measured using volumetric analysis of the $CO_2$ released by a 6 M HCl solution [23].

### *2.4. X-ray Powder Diffraction Data Collection*

X-ray powder diffraction (XRD) analyses were performed on the powdered soil samples collected at the 15–30 cm depth from each site at the farms in order to identify the main phases of the soil that were less disturbed by anthropogenic activities. Before proceeding with the analyses, for each soil sample, an aliquot of powder was dried at 60 °C overnight to remove the hygroscopic water. Data collection was performed using a Bruker D8 Advance Da Vinci diffractometer working in Bragg–Brentano geometry equipped with a LynxEye XE silicon strip detector (angular range of the detector window size = 2.585° 2θ) set to discriminate Cu Kα1,2 radiation, and a Ni-filter to suppress Cu Kβ component. The powder was placed on a zero-background sample holder and scanned in a continuous mode from 3 to 80° 2θ with a step size of 0.02° 2θ and a counting time of 5 s per step. Qualitative phase analysis of collected patterns was performed using Bruker AXS EVA software (v.5). Semi-quantitative analysis was performed using Profex software (version 4.3.6) [24].

### *2.5. Geochemical Analyses*

#### 2.5.1. Carbon Elemental Analysis and Carbon Speciation

The C fraction contents (expressed in wt%) were measured from the powdered soil samples using an Elementar SoliTOC Cube analyzer (Elementar©, Hanau, Germany) at CREA (Council for Agricultural Research and Economics, Institute of Gorizia, Italy). Homogenous powdered samples (around 100 mg) were weighed in stainless steel crucibles and placed in an autosampler. The analysis was carried out with a "smart combustion" method [25], which involves a three-step heating of the samples to 400, 600, and 900 °C with holding times of 230, 120, and 150 s, respectively, in order to measure different C fractions: (i) the thermally labile organic carbon ($TOC_{400}$) stripped out at temperatures below 400 °C, (ii) the residual oxidizable carbon (ROC) at temperatures of 500–600 °C, and (ii) the total inorganic carbon (TIC) derived from the thermal breakdown of carbonate minerals at 650–850 °C. The total carbon (TC) was calculated using the instrument as the sum of TOC and TIC. A standard of calcium carbonate ($CaCO_3$, Calciumcarbonat, Elementar) and a soil standard (Bodenstandard, Elementar with approximately 1.3% C content) were analyzed before, between, and after each run. Repeated analyses of standard and soil-certified accuracy and precision better than 5% of the measured concentration were followed as per Natali et al. [26].

#### 2.5.2. Carbon Isotopic Analysis

Carbon isotope ratios ($^{13}C/^{12}C$) were determined with an elemental analyzer (EA) Vario Micro Cube (Elementar©, Hanau, Germany) coupled with an isotope ratio mass spectrometer (IRMS) Isoprime 100 (Isoprime©, Manchester, UK) at the Department of Physics and Earth Science of University of Ferrara (Italy), following the procedure described by Natali and Bianchini [27] and Natali et al. [28]. Homogenous powdered samples (up to 40 mg) were weighed and wrapped in tin capsules and burned at 950 °C for the isotopic analyses of total carbon ($\delta^{13}C_{TC}$) and at 500 °C for the isotopic analyses of organic carbon ($\delta^{13}C_{TOC}$). Isotope ratio is expressed following isotope signature δ notation (in ‰):

$$\delta = (\delta R_{sample}/\delta R_{standard} - 1) \times 1000$$

where $R_{sample}$ is the isotopic ratio $^{13}C/^{12}C$ of the sample and $R_{standard}$ is the isotopic ratio $^{13}C/^{12}C$ of the Vienna Pee Dee Belemenite (V-PDB) international standard [29].

Calibration of the instrument was carried out using several standards: limestone JLs-1 [30], Carrara Marble [27], Jacupiranga carbonatite [31], and caffeine IAEA-600. As defined using repeated analyses of selected samples, the isotopic $\delta^{13}C_{TC}$ and $\delta^{13}C_{TOC}$ values had an average standard deviation (1σ) of ±0.1‰ and ±0.3‰, respectively.

#### 2.5.3. Nitrogen Elemental Analysis

The N contents (expressed in wt%) were measured from the powdered soil samples using the EA Vario Micro Cube (Elementar©, Hanau, Germany) at the Department of Physics and Earth Science of the University of Ferrara (Italy). Up to 40 mg of the powdered sample was wrapped in tin capsules and combusted at 950 °C in the EA to release $NO_x$ gases in the combustion tube. The gases are transferred into the reduction tube filled with native copper to remove the excess of oxygen and convert $NO_x$ species into $N_2$. Finally, the N contents were quantitatively determined using a thermo-conductivity detector (TCD). Calibration of the instrument was carried out using two standards: caffeine IAEA-600 and peach leaves NIST SRM1547 [32]. The precision of elemental concentration measurement was estimated using repeated analyses of the standards, and accuracy was estimated using a comparison between the reference and measured values, which was in the order of 5% of the absolute measured value. Uncertainties increase for contents approaching the detection limit (0.001 wt%).

### *2.6. Statistical Data Analysis*

Statistical analyses were performed using the R environment (R version 4.0.2 [33]). One-way analysis of variance (ANOVA) and Tukey's HSD post hoc tests were applied to each C fraction, total nitrogen, and C isotopes to determine statistical differences among the soil samples collected in 2020 and 2021 within each farm. For all statistical tests, the cutoff value was set at $p < 0.05$, which indicated significant differences between the groups. Correlation plots were used to investigate possible relationships among the C pools and isotopic parameters.

## 3. Results

### *3.1. Soil Texture and Physicochemical Properties*

The physicochemical characteristics of the soil profiles from the two farms are reported in Table 2.

**Table 2.** Values of pH, electric conductivity (EC), $CaCO_3$, clay, sand, and silt contents in the soil horizons of the soil profiles in the sites at the Branchicciolo and Beghelli farms.

| Site | Horizon | Depth (cm) | pH | EC ($\mu S\ cm^{-1}$) | $CaCO_3$ ($g\ kg^{-1}$) | Sand ($g\ kg^{-1}$) | Silt ($g\ kg^{-1}$) | Clay ($g\ kg^{-1}$) |
|---|---|---|---|---|---|---|---|---|
| ***Branchicciolo*** | | | | | | | | |
| **BRA 1** | Oi | 4–0 | n.d. | n.d. | n.d. | n.d. | n.d. | n.d. |
| | A1 | 0–5 | 7.6 | 426 | 107 | 827 | 168 | 5 |
| | A2 | 5–10.5 | 7.7 | 328 | 140 | 762 | 222 | 16 |
| | AB | 10.5–20.5 | 7.5 | 259 | 189 | 679 | 315 | 6 |
| | Bw | 20.5–33.5 | 7.1 | 200 | 229 | 703 | 231 | 66 |
| | BC | 33.5–40+ | n.d. | n.d. | n.d. | n.d. | n.d. | n.d. |
| **BRA 2** | Oi | 4–0 | n.d. | n.d. | n.d. | n.d. | n.d. | n.d. |
| | Oe | 0–1 | n.d. | n.d. | n.d. | n.d. | n.d. | n.d. |
| | A/Oe | 0–2/3 | 7.9 | 285 | 124 | 810 | 158 | 32 |
| | A | 2/3–11/12 | 7.8 | 293 | 166 | 684 | 252 | 64 |
| | Bw | 11/12–31 | 7.9 | 204 | 229 | 707 | 224 | 69 |
| | BC | 31–44 | 7.8 | 195 | 222 | 701 | 239 | 60 |
| **BRA 3** | Oi | 3–0 | n.d. | n.d. | n.d. | n.d. | n.d. | n.d. |
| | Oe | 0–2/3 | n.d. | n.d. | n.d. | n.d. | n.d. | n.d. |
| | A | 2/3–16 | 7.6 | 280 | 173 | 729 | 210 | 61 |
| | Bw | 16–30 | 7.7 | 189 | 213 | 742 | 160 | 97 |
| | BC1 | 30–46/49 | 7.7 | 205 | 211 | 677 | 220 | 103 |
| | BC2 | 46/49–66+ | 7.9 | 195 | 226 | 651 | 234 | 115 |

**Table 2.** *Cont.*

| Site | Horizon | Depth (cm) | pH | EC ($\mu S\ cm^{-1}$) | $CaCO_3$ ($g\ kg^{-1}$) | Sand ($g\ kg^{-1}$) | Silt ($g\ kg^{-1}$) | Clay ($g\ kg^{-1}$) |
|---|---|---|---|---|---|---|---|---|
| ***Branchicciolo*** | | | | | | | | |
| **BRA 4** | Oe | 0–1 | n.d. | n.d. | n.d. | n.d. | n.d. | n.d. |
| | A | 1–2 | 7.6 | 364 | 56 | 767 | 203 | 29 |
| | AB | 2–7 | 7.4 | 272 | 127 | 645 | 276 | 79 |
| | Bw1 | 7–15 | 7.6 | 255 | 144 | 677 | 246 | 77 |
| | Bw2 | 15–27 | 7.8 | 222 | 167 | 586 | 309 | 105 |
| | BC | 27–37 | 7.8 | 213 | 178 | 555 | 342 | 103 |
| ***Beghelli*** | | | | | | | | |
| **BEG 1** | Oi | 2–0 | n.d. | n.d. | n.d. | n.d. | n.d. | n.d. |
| | Oe | 0–1 | n.d. | n.d. | n.d. | n.d. | n.d. | n.d. |
| | A | 1–7 | 6.9 | 258 | 111 | 507 | 434 | 59 |
| | Bw | 7–24 | 7.1 | 298 | 36 | 370 | 355 | 275 |
| | BC | 24–37 | n.d. | n.d. | n.d. | n.d. | n.d. | n.d. |
| **BEG 2** | Oi | 0.2–0 | n.d. | n.d. | n.d. | n.d. | n.d. | n.d. |
| | A1 | 0–4/5 | 5.6 | 191 | 0 | 582 | 337 | 81 |
| | A2 | 4/5–6/7 | 5.4 | 99 | 0 | 460 | 399 | 141 |
| | Bw | 6/7–21 | 4.9 | 70 | 0 | 315 | 450 | 235 |
| | BC1 | 21–36 | 5.9 | 89 | 0 | 334 | 383 | 283 |
| | BC2 | 36–51 | 5.7 | 98 | 0 | 347 | 258 | 395 |
| | C | 51–61+ | 7.4 | 180 | 0 | 504 | 180 | 316 |
| **BEG 3** | Oi | 0.5–0 | n.d. | n.d. | n.d. | n.d. | n.d. | n.d. |
| | Oe/Oa | 0–0.5 | 6.8 | 311 | 182 | n.d. | n.d. | n.d. |
| | AE | 0.5–4.5/7.5 | 6.3 | 150 | 0 | 294 | 468 | 238 |
| | AB | 4.5/7.5–23 | 6.9 | 279 | 0 | 255 | 500 | 245 |
| | Bw | 23–38 | 7.4 | 324 | 0 | 225 | 458 | 317 |
| | BC1 | 38–45 | 7.5 | 225 | 0 | 203 | 435 | 362 |
| | BC2 | 45–65+ | 7.0 | 144 | 0 | 235 | 439 | 326 |
| **BEG 4** | Oi | 2–0 | n.d. | n.d. | n.d. | n.d. | n.d. | n.d. |
| | A | 0–7 | 6.8 | 253 | 0 | 534 | 371 | 95 |
| | Bw1 | 7–18 | 6.3 | 58 | 0 | 214 | 532 | 254 |
| | Bw2 | 18–38 | 7.2 | 154 | 0 | 294 | 464 | 242 |
| | C | 38–49 | n.d. | n.d. | n.d. | n.d. | n.d. | n.d. |

n.d. = not determined.

The soil profiles from the BRA farm were quite homogeneous each other. The soils were mainly sandy loam; only the most superficial horizons at the BRA 1 and BRA 4 sites were loamy sand (Figure 3). The soils from BRA showed relatively high pH values (7.1–7.9), associated with a high concentration of carbonate (56–229 g $kg^{-1}$) due to the presence of limestone deposits in this area. The soil profiles from the BEG farm were homogenous with each other. The most superficial horizons were sandy loam, while the rest of the horizons showed a loam or clay loam texture (Figure 3). In the BEG sites, soil pH was from acidic to neutral (4.9–7.5), in accordance with the absence of carbonate. The EC values of the BRA soils (158 to 342 $\mu S\ cm^{-1}$) were slightly lower than the BEG soils (180 to 532 $\mu S\ cm^{-1}$).

### 3.2. Phase Identification

An example of X-ray powder diffraction patterns collected at room temperature for each farm is reported in Supplementary Figure S1, and the semiquantitative data for each sample are reported in Table 3. Irrespective of the area of provenance, in all the investigated samples, the main phase is quartz. The other common mineralogical phases include feldspars (albite and microcline) and phyllosilicates (muscovite, kaolinite, and illite in both farms plus chlorite in the BRA farm and paragonite and vermiculite in the BEG farm). However, phyllosilicates are less abundant in the BRA soils than in the BEG soils.

Only the BRA soils are characterized by the presence of calcite, as they are in an area with limestone–sandstone deposits. On the other hand, the BEG soils also contain clinoptilolite, an authigenic mineral of the zeolite group.

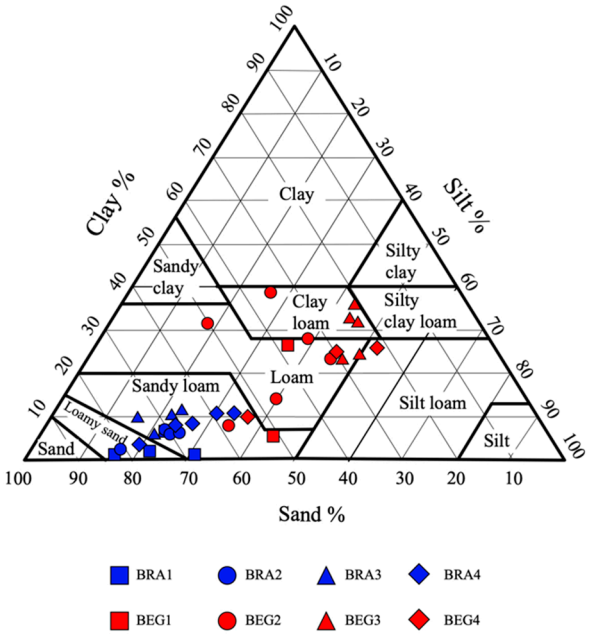


**Figure 3.** Soil texture samples of the BRA and BEG horizons collected in 2020 were plotted on the USDA (United States Department of Agriculture) triangle for soil texture classification.

**Table 3.** Contents and relative standard deviation of the main mineralogical phases of the composite soil samples collected at the fixed depth of 15–30 cm from the Branchicciolo (BRA) and Beghelli (BEG) farms in 2021.

| **Farm** | ***Branchicciolo*** | | | | | | | | ***Beghelli*** | | | | | |
|---|---|---|---|---|---|---|---|---|---|---|---|---|---|---|
| **Site** | **BRA 1** | | **BRA 2** | | **BRA 3** | | **BRA 4** | | **BEG 2** | | **BEG 3** | | **BEG 4** | |
| | wt% | | wt% | | wt% | | wt% | | wt% | | wt% | | wt% | |
| ***Quartz*** | 29.5 | ±0.4 | 33.4 | ±0.3 | 34.0 | ±0.3 | 33.9 | ±0.3 | 28.5 | ±0.3 | 30.7 | ±0.4 | 40.5 | ±0.4 |
| ***Feldspars*** | | | | | | | | | | | | | | |
| Albite | 8.3 | ±0.3 | 9.5 | ±0.3 | 11.5 | ±0.3 | 9.6 | ±0.3 | 9.4 | ±0.3 | 11.5 | ±0.3 | 13.5 | ±0.3 |
| Microcline | 8.0 | ±0.6 | 4.2 | ±0.3 | 6.8 | ±0.4 | 4.7 | ±0.4 | 9.9 | ±0.4 | 9.0 | ±0.5 | 10.5 | ±0.5 |
| ***Phyllosilicates*** | | | | | | | | | | | | | | |
| Muscovite | 6.8 | ±0.6 | 8.6 | ±0.5 | 11.6 | ±0.6 | 12.7 | ±0.6 | 20.5 | ±0.5 | 21.0 | ±0.6 | 4.3 | ±0.5 |
| Paragonite | --- | --- | --- | --- | --- | --- | --- | --- | 6.3 | ±0.3 | --- | --- | 7.9 | ±0.4 |
| Kaolinite | 3.5 | ±0.2 | 5.2 | ±0.4 | 8.0 | ±0.4 | 6.1 | ±0.4 | 15.5 | ±0.4 | 13.2 | ±0.5 | 6.6 | ±0.3 |
| Illite | 5.0 | ±0.7 | 8.4 | ±0.5 | 2.9 | ±0.6 | 6.7 | ±0.6 | 3.5 | ±0.5 | 7.0 | ±0.6 | 6.7 | ±0.6 |
| Chlorite | 9.1 | ±0.7 | 6.4 | ±0.5 | 4.7 | ±0.4 | 4.8 | ±0.4 | --- | --- | --- | --- | 4.3 | ±0.1 |
| Vermiculite | --- | --- | --- | --- | --- | --- | --- | --- | 2.1 | ±0.1 | 1.6 | ±0.1 | 0.6 | ±0.1 |
| ***Carbonates*** | | | | | | | | | | | | | | |
| Calcite | 29.8 | ±0.4 | 24.3 | ±0.2 | 20.4 | ±0.3 | 21.5 | ±0.2 | --- | --- | --- | --- | --- | --- |
| ***Zeolites*** | | | | | | | | | | | | | | |
| Clinoptilolite | --- | --- | --- | --- | --- | --- | --- | --- | 4.4 | ±0.2 | 6.0 | ±0.3 | 5.0 | ±0.2 |

### *3.3. Soil Carbon and Nitrogen Elemental Contents and Carbon Isotopic Ratios*

The average contents of TC, IC, TOC, and N in the 0–15 cm and 15–30 cm soil layers from the BRA and BEG farms in 2020 and 2021, as well as the respective isotopic ratios, are shown in Figure 4. The data related to the individual sites are reported in Supplementary Table S1.

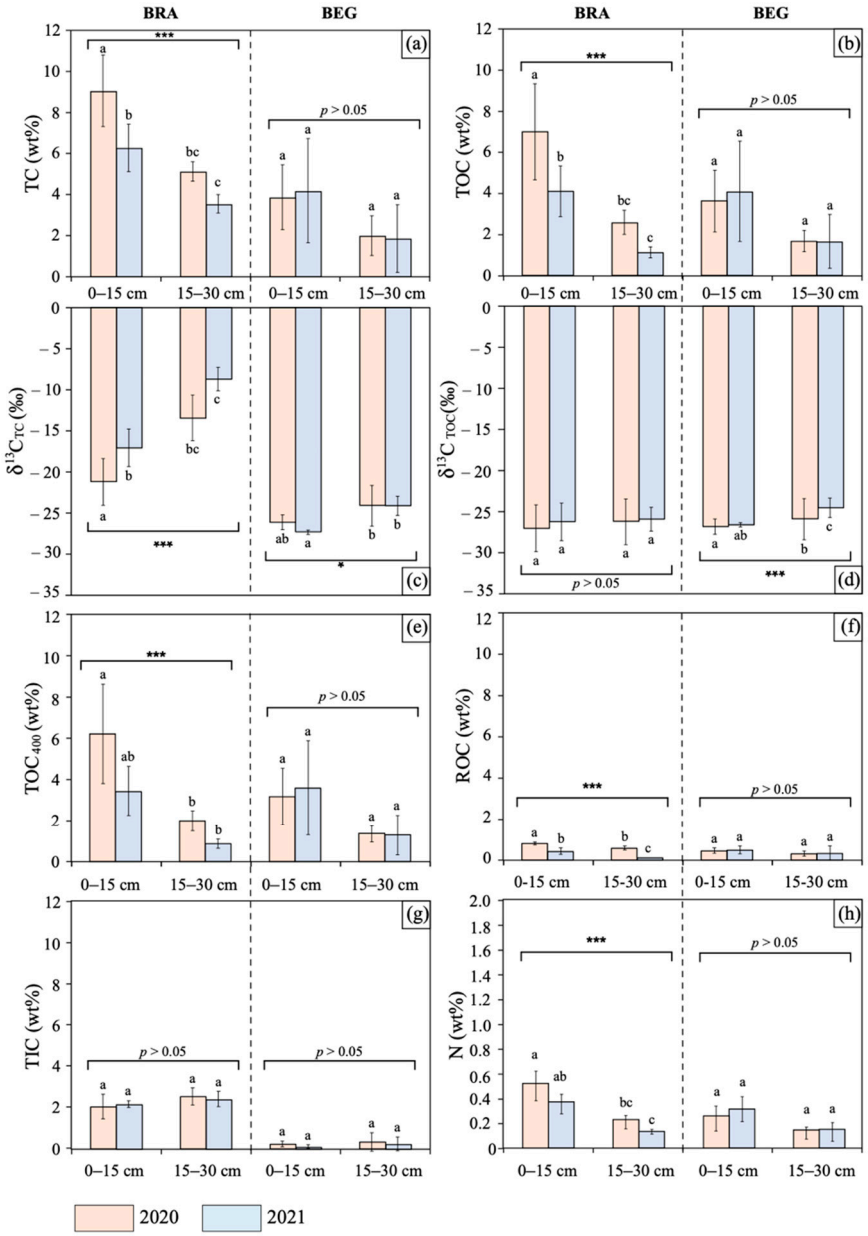


**Figure 4.** Average contents of the total (TC), inorganic (TIC), organic (TOC), labile organic ($TOC_{400}$), and residual oxidizable (ROC) carbon and nitrogen (N), as well as the isotopic signature of TC ($\delta^{13}C_{TC}$) and TOC ($\delta^{13}C_{TOC}$) in the soil samples collected at 0–15 and 15–30 cm soil depths from the Branchicciolo (BRA) and Beghelli (BEG) farms in 2020 and 2021. The error bars are the standard deviations. A one-way ANOVA was applied to each parameter considered for the BRA and BEG forests separately, and the results were also reported (* $p < 0.01$; *** $p < 0.0001$); where the asterisks are missing, the groups are not statistically different ($p > 0.05$). Different lowercase letters represent significant differences ($p < 0.05$) among the layers in 2020 and 2021, according to Tukey's HSD post hoc test applied to the BRA and BEG forests separately.

The ANOVA and Tukey's HSD post hoc tests showed that in the BRA soil, the contents of all the C fractions and $\delta^{13}C_{TC}$ and $\delta^{13}C_{TOC}$ were significantly affected by the year and depth of sampling ($p < 0.0001$). The only exception was found in the inorganic pool. In detail, for the BRA farm, both in 2020 and 2021, the topsoil (0–15 cm) was characterized by higher TC elemental contents than the subsoil (15–30 cm) coupled with more negative $\delta^{13}C_{TC}$. However, in one year, the TC contents decreased, and the isotopic ratios became less negative at all depths (Figure 4a,c). The TIC contents from the BRA farm were lower in the topsoil than in the subsoil in 2020 and 2021 and did not change significantly in one year (Figure 4g). On the contrary, the C contents in the organic fractions (i.e., TOC, $TOC_{400}$, ROC) from the BRA farm were higher in the topsoil than in the subsoil in both years and strongly decreased from 2020 to 2021 at all depths (Figure 4b,e,f). Noteworthy, the organic C fraction prevailed over the inorganic C fraction, and the labile organic carbon was much higher than the residual oxidizable carbon both in the topsoil and subsoil. The isotopic fingerprint of the organic fraction was referred to as TOC (Figure 4d). Overall, the TOC isotopic values did not change significantly with depth in both years, as they became slightly less negative from the topsoil to subsoil (Figure 4d). In addition, the TOC isotopic fingerprints of the topsoil and subsoil had less negative values from 2020 to 2021 (Figure 4d). Finally, the N contents are always higher in the topsoil and subsoil. However, the N contents were low in both years, with 2020 recording the highest values (Figure 4h). A different situation occurred at the BEG farm. According to the ANOVA and Tukey's HSD post hoc tests, for the BEG soil, the contents of all the C pools and N were statistically very similar ($p > 0.05$) among the years; only $\delta^{13}C_{TC}$ ($p < 0.01$) and $\delta^{13}C_{TOC}$ ($p < 0.0001$) were affected by the year of sampling. At the BEG farm, the topsoil had higher TC content and a more negative $\delta^{13}C_{TC}$ value than the subsoil both in 2020 and 2021 (Figure 4a,c). One year after the first sampling, the TC content increased in the topsoil and had a more negative isotopic value, whereas TC decreased in the subsoil without any change in the isotopic fingerprint (Figure 4a,c). The TIC content was lower in the topsoil than in the subsoil in both years; however, the TIC content did not change from 2020 to 2021 at any depth (Figure 4g). The TOC, $TOC_{400}$, and ROC contents always had the highest values in topsoil, and these values increased with time (Figure 4b,e,f). On the other hand, the TOC, $TOC_{400}$, and ROC contents in subsoil remained stable (Figure 4b,e,f). Regarding the BRA soils, in this case, the organic C fraction was higher than the inorganic C fraction, and the labile organic carbon was much higher than the residual oxidizable carbon both in the topsoil and subsoil. Regarding the TOC isotopic fingerprint, the values were always more negative in the topsoil than in the subsoil (Figure 4d). However, the $\delta^{13}C_{TOC}$ values became less negative both in the topsoil and subsoil in one year (Figure 4d). Finally, the N contents were low in both years and mirrored the trend in TOC and $TOC_{400}$, with the highest N content in the topsoil, which also slightly increased from 2020 to 2021, whereas the N content in the subsoil did not record any changes with time (Figure 4h).

## 4. Discussion

### *4.1. Variation in C and N Contents and C Isotopic Ratios in the BRA Soil over Time*

At the BRA farm, the organic C fractions (i.e., TOC, $TOC_{400}$, and ROC) decreased with depth and time, while TIC did not record significant changes, reflecting the relatively high carbonate contents (Table 2) of the limestone–sandstone deposits in the area (Figure 1b). This was also confirmed by the presence of calcite in the XRD patterns of all BRA samples. In detail, in the BRA topsoil (0–15 cm), most of the C was included in the most labile organic fraction (i.e., $TOC_{400}$), which is commonly related to untransformed organic matter [26]. Only a limited amount of C is preserved as ROC, i.e., the C fraction with a longer turnover. In both years, the amount of $TOC_{400}$ decreased with depth while remaining the predominant OC fraction. In general, subsoils tend to contain a substantial portion of stored soil OC in more protected forms [34], which was detected as ROC during the analyses [26]. However, in this case, both $TOC_{400}$ and ROC contents decreased significantly in one year in the topsoil and subsoil, which testifies to the scarce preservation of organic matter. Such

a trend was also observed for N, which confirms the organic matter loss, as this element is mainly hosted in organic substances. In mountain forests, rapid organic matter loss is normally associated with erosion processes, which mainly affect the most superficial horizons [35,36]. This phenomenon can be enhanced by intensive silvicultural practices [35] and/or intensive rainfall [37]. In the BRA farm, the highest C and N losses were recorded in the soil samples collected from the BRA 4 site (Table S1), which is located in the steepest zone (45% slope; Table 1) of the study site and, therefore, it is vulnerable to erosion processes. However, the BRA 2 and BRA 3 sites, which were characterized by low slopes (5% and 3%, respectively), also recorded a strong decrease in organic C fractions and N (Table S1). In these latter sites, the erosion processes cannot cause strong organic matter loss in one year; therefore, other anthropic and/or natural causes should be considered. Silviculture practices could have a role in this phenomenon; however, the removal of 25% of the stem cannot be the only reason for the SOC depletion recorded in the BRA forest. Climate conditions, namely, temperature and precipitation, are other important factors that affect the sequestration of organic C. Indeed, soil OC accumulation and sequestration are favored in cold and humid areas rather than in hot and dry regions [38–40]. Since the BRA soils are located at a lower altitude compared with the BEG soils, the temperature is warmer and, combined with the reduced amount of aboveground plant biomass for the drought, this could have promoted SOM depletion. This trend was also exacerbated by the slope of the BRA forest toward the southwest, i.e., having maximum sun exposure, which implies an increase in soil temperature, and consequently, soil evaporation [41]. The higher temperatures could have enhanced microbial activity and, therefore, accelerated SOM decomposition, as demonstrated by the decrease in $TOC_{400}$ and ROC in both the topsoil and subsoil (Figures 4e,f and 5a). The limited supply of C input could have exacerbated this situation, as the soil microorganisms could have also decomposed the more stable organic matter (i.e., ROC) in the BRA soil. Accordingly, the isotopic signatures related to the total ($\delta^{13}C_{TC}$) and organic ($\delta^{13}C_{TOC}$) C fractions in the BRA topsoil and subsoil were more negative in 2020 rather than in 2021 (Figure 4c,d). The depletion of $\delta^{13}C_{TC}$ over time reflects the lower amount of organic material in both the topsoil and subsoil, which is difficult to explain as it could be related to (i) erosion phenomena, which removed the most superficial materials and/or (ii) higher temperatures, which triggered isotopic fractionation processes promoting $^{12}C$ emission into the atmosphere. Also, the $\delta^{13}C_{TOC}$ in the topsoil and subsoil was slightly less negative in 2021 than in 2020, which further confirms the enhancement of mineralization processes [42,43].

### *4.2. Variation in C and N Contents and C Isotopic Ratios in BEG Soil over Time*

In the BEG soil, the TC and all organic fractions decreased from the topsoil to the subsoil both in 2020 and 2021. However, in one year, these C contents slightly increased in the topsoil, especially $TOC_{400}$, which is indicative of organic matter input, e.g., from plant residues on the forest floor (Figure 5b). Accordingly, the $\delta^{13}C_{TC}$ in the topsoil in 2021 was slightly more negative, whereas the TC isotopic signatures of the subsoil and those of OC in the BEG soils remained similar over time. The absence of any variations in C contents and signatures indicates that this area was not affected by the erosion process, despite it being characterized by a steep slope (slope gradient 20–45%). In addition, it was not affected by the loss of organic matter due to silviculture management, despite the removal of 60% of forest material (i.e., stems, understory bushes, small and low-quality trees). The preservation of organic matter was likely promoted by: (i) the colder mean air temperatures occurring in BEG compared with BRA; (ii) the selection of the period for the second sampling of BEG (September), when the vegetative period was concluding and most organic input was expected; (iii) the altitude, which slowed down SOC decomposition rates [44–46]; and (iv) the shady slope, as the BEG forest was exposed toward the north, which guarantees higher soil moisture and lower soil temperature contents compared with sunny slopes, like those in the BRA forest, even during droughts [41]. Another important factor of the SOC stock is the soil texture, considering the SOM stabilization capacity of minerals with reactive

mineral surface areas. The texture of the BEG soil was clay loam/loam, characterized by the presence of authigenic secondary phyllosilicates, including clays and zeolite minerals. Such texture is more favorable for sequestering and protecting organic matter in more stable forms than the sandy BRA soil (Figure 4). According to Tian and He [47], temperature affects the amount of litter but has no effect on OC stability. In fact, the stabilization of OC is determined by the interaction with soil minerals, which makes the organic matter inaccessible to decomposer organisms [48]. In this case, SOM can be protected and can persist over long time scales [49,50] in recalcitrant forms (i.e., ROC). It is well known that clays and zeolites adsorb a greater quantity of OC and have high stabilization capacity due to their large specific surface area (SSA) and their cation exchange capacity (CEC), i.e., the measure of layer charge in minerals [51–54]. According to the texture analyses (Table 2) and mineralogical analyses (Table 3, Figure S1), the BEG soils have higher clay and zeolite contents than the BRA soils. Therefore, the BEG soils were more prone to stabilize the OC in recalcitrant form, preserving the organic matter from degradation. It is important to clarify that clay minerals have different stabilization capacities [53,55]. For clay, the 2:1 type phyllosilicates (e.g., vermiculite and iilite) adsorb a greater quantity of OC in soil than the 1:1 type clay minerals (e.g., kaolinite), as the formers contain a larger amount of SSA and CEC than the latter [53]. In this case, only the BEG soils were characterized by the presence of vermiculite, which is considered the clay mineral with the highest ability to stabilize SOC, as it is characterized by the highest SSA and CEC among the phyllosilicates [51,54]. Similarly, among natural zeolites, clinoptinolite, which was hosted in the BEG soil, has exceptionally high CEC, which guarantees organic carbon sequestration in soil [56]. Therefore, the mineralogical composition of the BEG soils contributes to organic matter preservation.

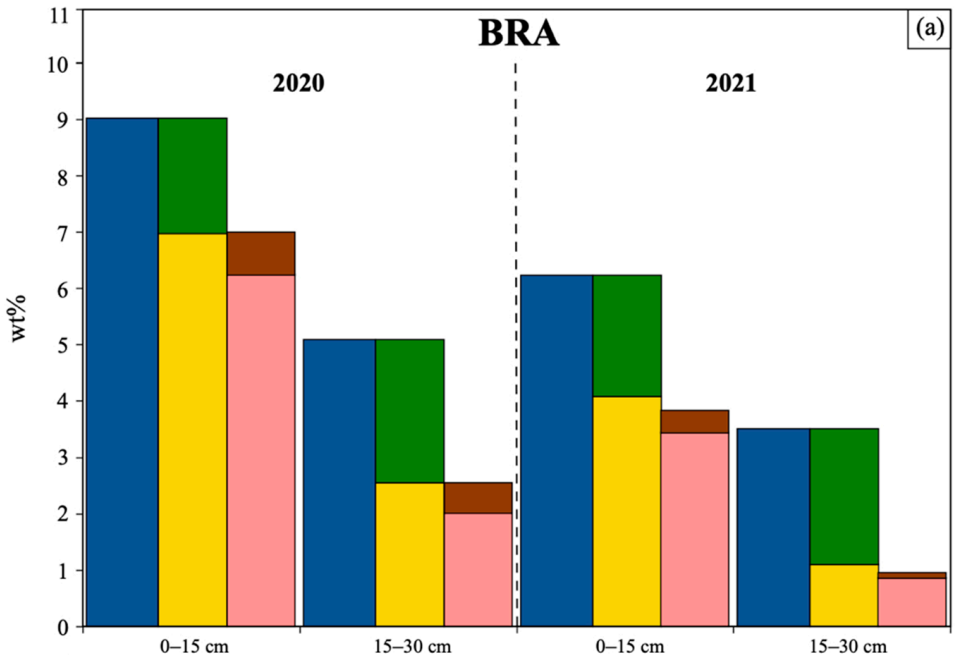


**Figure 5.** *Cont.*

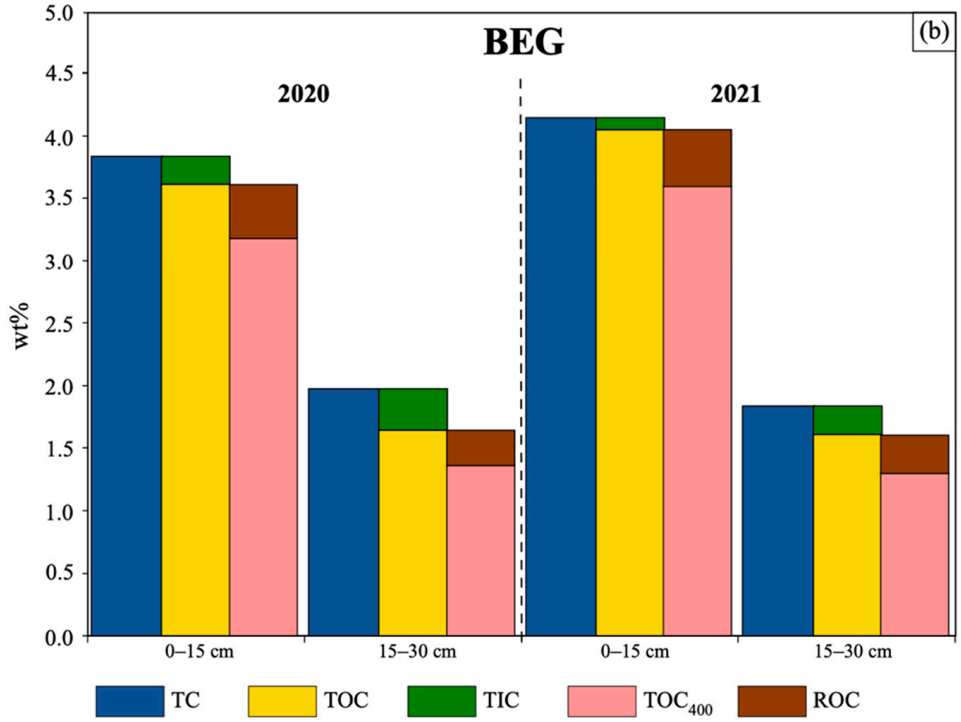


**Figure 5.** Average elemental contents of the total (TC), inorganic (TIC), organic (TOC), labile organic ($TOC_{400}$), residual oxidizable (ROC) carbon in 0–15 and 15–30 cm layers from the (**a**) BRA and (**b**) BEG farms in 2020 and 2021.

### *4.3. Comparison between the Farms*

Figure 6 presents an analysis of the relationship between the soil geochemical variables considered in this study, i.e., C and N contents and the relative isotopic fingerprints for the BRA and BEG farms in 2020 and 2021. According to the plots, the C in the soil is mostly related to the organic matter at both farms, as there is a strong correlation between the TC and TOC contents ($R^2$ = 0.90), and in particular with $TOC_{400}$ ($R^2$ = 0.88). This is not surprising, as it is well known that on the forest floor, the principal source of "fresh" organic matter is dead plant material (litter), followed by rhizodeposits (i.e., exudates from plant roots), fecal material, and bodies of the soil biota [5]. Such organic materials are progressively decomposed by soil fauna and microorganisms (fungi, bacteria, and arches), which release a portion of C as $CO_2$ through respiration and transform the remnants into microbial biomass. After that, C is converted into microbial products, which can be bonded to the surface of clay minerals, thus protecting C from decomposition for a long period [5,52] and creating stable soil C (or ROC), which is preserved in general at higher depths (i.e., >15 cm) [26]. In Figure 6, the TC contents shows a good correlation with the ROC contents ($R^2$ = 0.75). In addition, it also highlights the loss in ROC contents from the BRA soils from 2020 to 2021, whereas, in the BEG soils, the difference between the years is not as evident, despite the removal of 60% of forest material during the annual thinning intervention (much more than what was removed in the same time in the BRA forest). Here, the mineral clays and zeolites in the soils could have played an important role in preserving the organic matter from decomposition.

In summary, the BRA farm recorded more OC contents than the BEG farm both in 2020 and 2021 (Figures 4 and 5). The average OC contents in the BRA soil decreased rapidly, probably due to the combined effects of higher mean air temperatures compared with BEG and the reduced amount of vegetation biomass. On the other hand, the average OC contents in the BEG soil were almost stable in one year due to (i) the colder temperature, typical of higher altitude and the sampling period in 2021 (September) and (ii) the predominance of authigenic secondary phyllosilicate (including vermiculite) and zeolite (clinoptinolite) minerals.

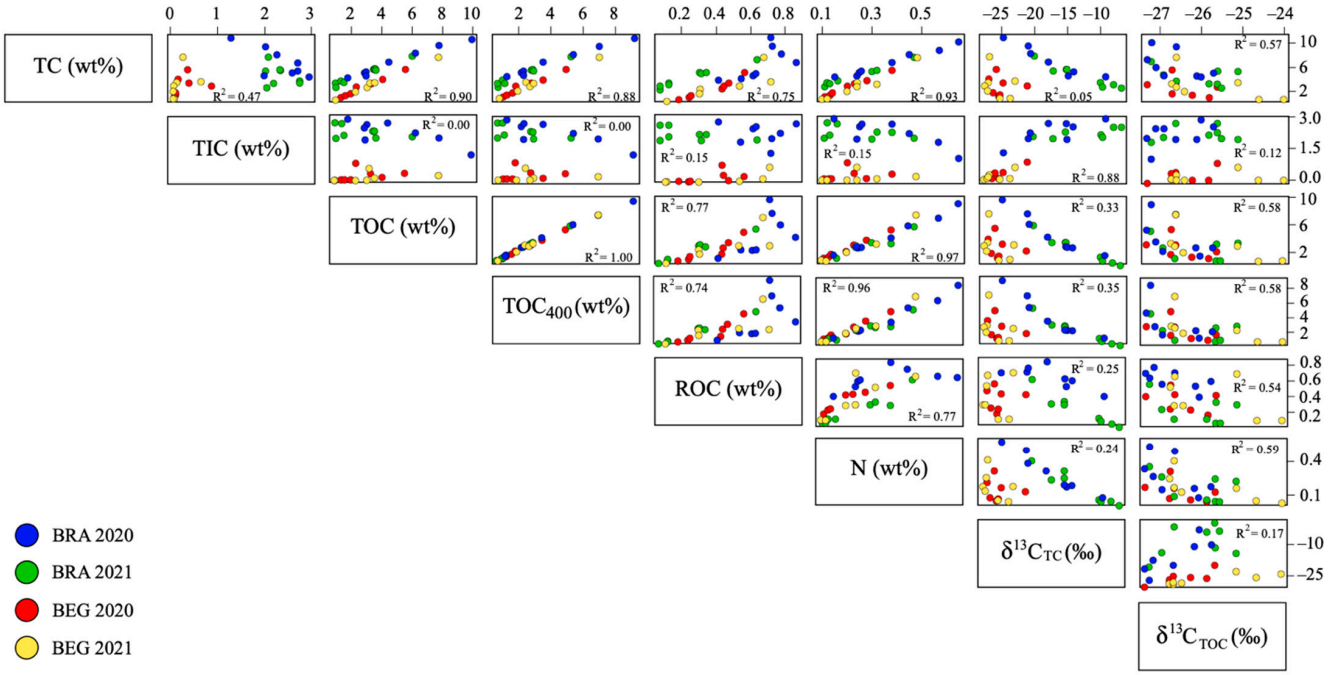


**Figure 6.** Correlation plots for elemental contents in the total (TC), inorganic (TIC), organic (TOC), labile organic ($TOC_{400}$), residual oxidizable (ROC) carbon, and isotopic ratios $\delta^{13}C_{TC,}$ $\delta^{13}C_{TOC}$ in 0–15 and 15–30 cm layers from the sites at the BRA and BEG farms in 2020 and 2021.

## 5. Conclusions

The central interface of Earth's critical zone is soil, which carries out several ecosystem services, including carbon (C) sequestration, is fundamental for the fertility of the area as well as for reducing greenhouse gases (e.g., $CO_2$) in the atmosphere. Forest soil has the highest C sequestration capacity; therefore, understanding its dynamics and the influence of natural (e.g., climate and soil texture) and anthropic (e.g., silvicultural management) factors is fundamental for the mitigation of climate change. This work investigated the capacity of C sequestration into soils from two temperate forests in the Apennine Mountain area (Emilia-Romagna; Italy) managed with silvicultural practices by two farms. Despite the Branchicciolo (BRA) and Beghelli (BEG) farms being located only 15 km apart, they experienced different situations in a span of only one year. The BRA soil had more C fractions than the BEG soil in 2020. However, after only one year, the situation changed drastically. The BRA soil recorded strong decreases in the TC and OC fractions, and the relative isotopic signature became less negative, indicating a loss in organic matter. On the contrary, in the BEG soil, all the C fractions and the related isotopic signature remained stable over time. It is important to investigate the potential reasons for these opposite trends in the two nearby farms, which cannot be related to the silvicultural management, as much more forest material was removed from the BEG forest than in the BRA forest (60% and 25%, respectively). We ignored the effects of erosional processes considering that some of the BRA sampling sites, recording loss of organic matter, were in approximatively flat areas. However, the two farms differed from each other in altitude, soil texture, and composition: these are important factors for organic C sequestration in forest soil. Among the two farms, there was an altitude difference of about 300 m, which may have created different micro-climate conditions. The BEG forest was located at a higher altitude than the BRA forest. Thus, the colder temperature could have promoted C preservation. A crucial role was also played by the different soil textures at the two farms. Phyllosilicates, in particular clays, and zeolites are predominant in the BEG clay loam/loam soils and not in the BRA sandy soils. These minerals are characterized by high specific surface area and cation exchange capacity, which promotes SOC sequestration and protects the organic matter fractions from

microbial decomposition. In addition, the BEG soils are characterized by the presence of vermiculite, a mineral with the highest capacity to sequester among phyllosilicates.

This work shed light on the importance of detailed knowledge of the local pedo-climatic conditions of an area, even at the mineralogical scale, which can differ substantially in a relatively restricted portion of territory and create opposite trends for OC sequestration. In this way, forest farmers and the local and national authorities can plan the most appropriate silvicultural management to favor OC sequestration, or at least, to contrast SOM degradation. The effects of organic matter loss in forests will be devasting, as these environments represent one of the largest sinks of C. Therefore, a loss of forests will lead to large disturbances to C cycle dynamics on a global scale, as well as the loss of ecological biodiversity.

**Supplementary Materials:** The following supporting information can be downloaded at: https://www.mdpi.com/article/10.3390/environments10090156/s1, Figure S1: 1. Examples of XRD patterns; Table S1: Elemental of the total (TC), inorganic (TIC), organic (TOC), labile organic ($TOC_{400}$), residual oxidizable (ROC) carbon, and nitrogen (N), as well as the isotopic signature of TC ($\delta^{13}C_{TC}$) and TOC ($\delta^{13}C_{OC}$) of the composite soil samples collected at the fixed depths of 0–15 and 15–30 cm in Branchicciolo (BRA) and Beghelli (BEG) farms in 2020 and 2021.

**Author Contributions:** Conceptualization, G.B.; methodology, V.B., G.M.S., M.D.F., E.M. and G.B.; software, V.B. and N.P.; formal analysis, V.B., G.M.S., M.D.F., E.M., N.P. and G.B.; investigation, V.B., M.D.F. and G.B.; data curation, V.B., M.D.F. and G.B.; writing—original draft preparation, V.B., M.D.F. and G.B.; writing—review and editing, V.B., M.D.F. and G.B.; supervision, G.B.; funding acquisition, G.B. All authors have read and agreed to the published version of the manuscript.

**Funding:** This research was funded by Rural Development Program (RDP; Programma di Sviluppo Rurale-PSR) 2014–2020 of the Emilia-Romagna region, grant number 5112640.

**Data Availability Statement:** The data presented in this study are available in the Supplementary material of this article.

**Acknowledgments:** The authors thank the farms "Beghelli" and "Branchicciolo", as well as "Confagricoltura di Bologna" that collaborated on the SuoBo project. The authors also thank Flavio Fornasier of CREA laboratories of Gorizia (Italy) for supporting the geochemical analyses. Finally, the authors thank the Editorial Office and all the reviewers for their criticism and suggestion to improve the early version of the manuscript.

**Conflicts of Interest:** The authors declare no conflict of interest.

## References

1. Banwart, S.A.; Nikolaidis, N.P.; Zhu, Y.-G.; Peacock, C.L.; Sparks, D.L. Soil Functions: Connecting Earth's Critical Zone. *Annu. Rev. Earth Planet. Sci.* **2019**, *47*, 333–359. [CrossRef]
2. Clunes, J.; Valle, S.; Dörner, J.; Martínez, O.; Pinochet, D.; Zúñiga, F.; Blum, W.E.H. Soil Fragility: A Concept to Ensure a Sustainable Use of Soils. *Ecol. Indic.* **2022**, *139*, 108969. [CrossRef]
3. Hatfield, J.L.; Sauer, T.J.; Cruse, R.M. Chapter One—Soil: The Forgotten Piece of the Water, Food, Energy Nexus. *Adv. Agron.* **2017**, *143*, 1–46.
4. Haygarth, P.M.; Ritz, K. The Future of Soils and Land Use in the UK: Soil Systems for the Provision of Land-Based Ecosystem Services. *Land Use Policy* **2009**, *26*, 187–197. [CrossRef]
5. Mayer, M.; Prescott, C.E.; Abaker, W.E.A.; Augusto, L.; Cécillon, L.; Ferreira, G.W.D.; James, J.; Jandl, R.; Katzensteiner, K.; Laclau, J.-P.; et al. Tamm Review: Influence of Forest Management Activities on Soil Organic Carbon Stocks: A Knowledge Synthesis. *For. Ecol. Manag.* **2020**, *466*, 118127. [CrossRef]
6. Lal, R. Soil Management for Carbon Sequestration. *S. Afr. J. Plant Soil* **2021**, *38*, 231–237. [CrossRef]
7. Lal, R. Soil Carbon Sequestration Impacts on Global Climate Change and Food Security. *Science* **2004**, *304*, 1623–1627. [CrossRef]
8. Lal, R. Restoring Soil Quality to Mitigate Soil Degradation. *Sustainability* **2015**, *7*, 5875–5895. [CrossRef]
9. Scharlemann, J.P.W.; Tanner, E.V.J.; Hiederer, R.; Kapos, V. Global Soil Carbon: Understanding and Managing the Largest Terrestrial Carbon Pool. *Carbon Manag.* **2014**, *5*, 81–91. [CrossRef]
10. Pan, Y.; Birdsey, R.A.; Fang, J.; Houghton, R.; Kauppi, P.E.; Kurz, W.A.; Phillips, O.L.; Shvidenko, A.; Lewis, S.L.; Canadell, J.G.; et al. A Large and Persistent Carbon Sink in the World's Forests. *Science* **2011**, *333*, 988–993. [CrossRef] [PubMed]
11. Santini, N.S.; Adame, M.F.; Nolan, R.H.; Miquelajauregui, Y.; Piñero, D.; Mastretta-Yanes, A.; Cuervo-Robayo, Á.P.; Eamus, D. Storage of Organic Carbon in the Soils of Mexican Temperate Forests. *For. Ecol. Manag.* **2019**, *446*, 115–125. [CrossRef]

12. Ameray, A.; Bergeron, Y.; Valeria, O.; Montoro Girona, M.; Cavard, X. Forest Carbon Management: A Review of Silvicultural Practices and Management Strategies across Boreal, Temperate and Tropical Forests. *Curr. For. Rep.* **2021**, *7*, 245–266. [CrossRef]
13. Köhl, M.; Lasco, R.; Cifuentes, M.; Jonsson, Ö.; Korhonen, K.T.; Mundhenk, P.; de Jesus Navar, J.; Stinson, G. Changes in Forest Production, Biomass and Carbon: Results from the 2015 Un Fao Global Forest Resource Assessment. *For. Ecol. Manag.* **2015**, *352*, 21–34. [CrossRef]
14. Zhou, R.; Zhang, Y.; Peng, M.; Jin, Y.; Song, Q. Effects of Climate Change on the Carbon Sequestration Potential of Forest Vegetation in Yunnan Province, Southwest China. *Forests* **2022**, *13*, 306. [CrossRef]
15. Deng, L.; Peng, C.; Kim, D.-G.; Li, J.; Liu, Y.; Hai, X.; Liu, Q.; Huang, C.; Shangguan, Z.; Kuzyakov, Y. Drought Effects on Soil Carbon and Nitrogen Dynamics in Global Natural Ecosystems. *Earth Sci. Rev.* **2021**, *214*, 103501. [CrossRef]
16. Boisvenue, C.; Running, S.W. Impacts of Climate Change on Natural Forest Productivity—Evidence since the Middle of the 20th Century. *Glob. Chang. Biol.* **2006**, *12*, 862–882. [CrossRef]
17. Blanco, J.A. Managing Forest Soils for Carbon Sequestration: Insights from Modeling Forests around the Globe. In *Soil Management and Climate Change*; Academic Press: Cambridge, MA, USA, 2018; pp. 237–252.
18. Teng, F.-Z.; Ma, L. Deciphering Isotope Signatures of Earth Surface and Critical Zone Processes. *Chem. Geol.* **2016**, *445*, 1–3. [CrossRef]
19. ARPAE. *Rapporto Idrometeoclima Emilia-Romagna: Dati 2020*; Arpae Emilia-Romagna: Bologna, Italy, 2021; p. 65.
20. ARPAE. *Rapporto Idrometeoclima Emilia-Romagna: Dati 2021*; Arpae Emilia-Romagna: Bologna, Italy, 2022; p. 69.
21. Schoeneberger, P.J.; Wysocki, D.A.; Benham, E.C. *Soil Survey Staff, Field Book for Describing and Sampling Soils, Version 3.0*; Natural Resources Conservation Service, National Soil Survey Center: Lincoln, NE, USA, 2012.
22. Gee, G.W.; Bauder, J.W. Particle Size Analysis. In *Methods of Soil Analysis: Part 1 Physical and Mineralogical Methods*; ASA and SSSA: Madison, WI, USA, 1986; Volume 9.
23. Loeppert, R.H.; Suarez, D.L. Carbonate and Gypsum. In *Methods of Soil Analysis: Part 3 Chemical Methods*; ASA and SSSA: Madison, WI, USA, 1996.
24. Doebelin, N.; Kleeberg, R. Profex: A Graphical User Interface for the Rietveld Refinement Program Bgmn. *J. Appl. Crystallogr.* **2015**, *48*, 1573–1580. [CrossRef]
25. Zethof, J.H.T.; Leue, M.; Vogel, C.; Stoner, S.W.; Kalbitz, K. Identifying and Quantifying Geogenic Organic Carbon in Soils—The Case of Graphite. *Soil* **2019**, *5*, 383–398. [CrossRef]
26. Natali, C.; Bianchini, G.; Carlino, P. Thermal Stability of Soil Carbon Pools: Inferences on Soil Nature and Evolution. *Thermochim. Acta* **2020**, *683*, 178478. [CrossRef]
27. Natali, C.; Bianchini, G. Thermally Based Isotopic Speciation of Carbon in Complex Matrices: A Tool for Environmental Investigation. *Environ. Sci. Pollut. Res. Int.* **2015**, *22*, 12162–12173. [CrossRef]
28. Natali, C.; Bianchini, G.; Vittori Antisari, L.; Natale, M.; Tessari, U. Carbon and Nitrogen Pools in Padanian Soils (Italy): Origin and Dynamics of Soil Organic Matter. *Geochemistry* **2018**, *78*, 490–499. [CrossRef]
29. Gonfiantini, R.; Stichler, W.; Rozanski, K. *Standards and Intercomparison Materials Distributed by the International Atomic Energy Agency for Stable Isotope Measurements, References and Intercomparison Materials for Stable Isotopes of Light Elements*; IAEA: Vienna, Austria, 1993.
30. Kusaka, S.; Nakano, T. Carbon and Oxygen Isotope Ratios and Their Temperature Dependence in Carbonate and Tooth Enamel Using a Gasbench II Preparation Device. *Rapid Commun. Mass. Spectrom.* **2014**, *28*, 563–567. [CrossRef]
31. Beccaluva, L.; Bianchini, G.; Natali, C.; Siena, F. The Alkaline-Carbonatite Complex of Jacupiranga (Brazil): Magma Genesis and Mode of Emplacement. *Gondwana Res.* **2017**, *44*, 157–177. [CrossRef]
32. Dutta, K.; Schuur, E.A.G.; Neff, J.C.; Zimov, S.A. Potential Carbon Release from Permafrost Soils of Northeastern Siberia. *Glob. Chang. Biol.* **2006**, *12*, 2336–2351. [CrossRef]
33. *Rstudio: Integrated Development Environment for R*; R Studio, PBC: Boston, MA, USA, 2011. Available online: https://posit.co/download/rstudio-desktop/ (accessed on 22 June 2020).
34. Jobbágy, E.G.; Jackson, R.B. The Vertical Distribution of Soil Organic Carbon and Its Relation to Climate and Vegetation. *Ecol. Appl.* **2000**, *10*, 423–436. [CrossRef]
35. Harden, C.P. Soil Erosion and Sustainable Mountain Development. *Mt. Res. Dev.* **2001**, *21*, 77–83. [CrossRef]
36. Stanchi, S.; Falsone, G.; Bonifacio, E. Soil Aggregation, Erodibility, and Erosion Rates in Mountain Soils (NW Alps, Italy). *Solid Earth* **2015**, *6*, 403–414. [CrossRef]
37. Guerra, C.A.; Rosa, I.M.D.; Valentini, E.; Wolf, F.; Filipponi, F.; Karger, D.N.; Xuan, A.N.; Mathieu, J.; Lavelle, P.; Eisenhauer, N. Global Vulnerability of Soil Ecosystems to Erosion. *Landsc. Ecol.* **2020**, *35*, 823–842. [CrossRef]
38. Wiesmeier, M.; Urbanski, L.; Hobley, E.; Lang, B.; von Lützow, M.; Marin-Spiotta, E.; van Wesemael, B.; Rabot, E.; Ließ, M.; Garcia-Franco, N.; et al. Soil Organic Carbon Storage as a Key Function of Soils—A Review of Drivers and Indicators at Various Scales. *Geoderma* **2019**, *333*, 149–162. [CrossRef]
39. Brombin, V.; Mistri, E.; De Feudis, M.; Forti, C.; Salani, G.M.; Natali, C.; Falsone, G.; Vittori Antisari, L.; Bianchini, G. Soil Carbon Investigation in Three Pedoclimatic and Agronomic Settings of Northern Italy. *Sustainability* **2020**, *12*, 10539. [CrossRef]
40. Zhang, K.; Dang, H.; Zhang, Q.; Cheng, X. Soil Carbon Dynamics Following Land-Use Change Varied with Temperature and Precipitation Gradients: Evidence from Stable Isotopes. *Glob. Chang. Biol.* **2015**, *21*, 2762–2772. [CrossRef] [PubMed]

41. Liu, B.; Yu, P.; Zhang, X.; Li, J.; Yu, Y.; Wan, Y.; Wang, Y.; Wang, X.; Liu, Z.; Pan, L.; et al. Transpiration Sensitivity to Drought in Quercus wutaishansea Mary Forests on Shady and Sunny Slopes in the Liupan Mountains, Northwestern China. *Forests* **2022**, *13*, 1999. [CrossRef]
42. Liu, Y.; Hu, C.; Hu, W.; Wang, L.; Li, Z.; Pan, J.; Chen, F. Stable Isotope Fractionation Provides Information on Carbon Dynamics in Soil Aggregates Subjected to Different Long-Term Fertilization Practices. *Soil Tillage Res.* **2018**, *177*, 54–60. [CrossRef]
43. Hogberg, P. $^{15}$N Natural Abundance in Soil-Plant Systems. *New Phytol.* **2008**, *137*, 179–203. [CrossRef]
44. Eshetu, E.Y.; Hailu, T.A.; Tejada Moral, M. Carbon Sequestration and Elevational Gradient: The Case of Yegof Mountain Natural Vegetation in North East, Ethiopia, Implications for Sustainable Management. *Cogent Food Agric.* **2020**, *6*, 1733331. [CrossRef]
45. Moser, G.; Leuschner, C.; Hertel, D.; Graefe, S.; Soethe, N.; Iost, S. Elevation Effects on the Carbon Budget of Tropical Mountain Forests (S Ecuador): The Role of the Belowground Compartment. *Glob. Chang. Biol.* **2011**, *17*, 2211–2226. [CrossRef]
46. De Feudis, M.; Cardelli, V.; Massaccesi, L.; Trumbore, S.E.; Vittori Antisari, L.; Cocco, S.; Corti, G.; Agnelli, A. Small Altitudinal Change and Rhizosphere Affect the SOM Light Fractions but Not the Heavy Fraction in European Beech Forest Soil. *Catena* **2019**, *181*, 104091. [CrossRef]
47. Tian, Q.; He, H.; Cheng, W.; Bai, Z.; Wang, Y.; Zhang, X. Factors Controlling Soil Organic Carbon Stability Along a Temperate Forest Altitudinal Gradient. *Sci. Rep.* **2016**, *6*, 18783. [CrossRef] [PubMed]
48. Georgiou, K.; Jackson, R.B.; Vindušková, O.; Abramoff, R.Z.; Ahlström, A.; Feng, W.; Harden, J.W.; Pellegrini, A.F.A.; Polley, H.W.; Soong, J.L.; et al. Global stocks and capacity of mineral-associated soil organic carbon. *Nat. Commun.* **2022**, *13*, 3797. [CrossRef]
49. Calero, J.; García-Ruiz, R.; Torrús-Castillo, M.; Vicente-Vicente, J.L.; Martín-García, J.M. Role of Clay Mineralogy in the Stabilization of Soil Organic Carbon in Olive Groves under Contrasted Soil Management. *Minerals* **2023**, *13*, 60. [CrossRef]
50. Islam, M.R.; Singh, B.; Dijkstra, F.A. Stabilisation of soil organic matter: Interactions between clay and microbes. *Biogeochemistry* **2022**, *160*, 145–158. [CrossRef]
51. Singh, M.; Sarkar, B.; Sarkar, S.; Churchman, J.; Beerling, D.J. Stabilization of soil organic carbon as influenced by clay mineralogy. *Adv. Agron.* **2017**, *148*, 33–84.
52. Sarkar, B.; Singh, M.; Mandal, S.; Churchman, G.J.; Bolan, N.S. Clay Minerals—Organic Matter Interactions in Relation to Carbon Stabilization in Soils. In *The Future of Soil Carbon Its Conservation and Formation*; Garcia, C., Nannipieri, P., Hernandez, T., Eds.; Academic Press: Cambridge, MA, USA, 2018; pp. 71–86.
53. Doni, S.; Gispert, M.; Peruzzi, E.; Macci, C.; Mattii, G.B.; Manzi, D.; Masini, C.M.; Grazia, M. Impact of Natural Zeolite on Chemical and Biochemical Properties of Vineyard Soils. *Soil Use Manag.* **2020**, *37*, 832–842. [CrossRef]
54. Xue, B.; Huang, L.; Li, X.; Lu, J.; Gao, R.; Kamran, M.; Fahad, S. Effect of Clay Mineralogy and Soil Organic Carbon in Aggregates under Straw Incorporation. *Agronomy* **2022**, *12*, 534. [CrossRef]
55. Rasmussen, C.; Heckman, K.; Wieder, W.R.; Keiluweit, M.; Lawrence, C.R.; Berhe, A.A.; Blankinship, J.C.; Crow, S.E.; Druhan, J.L.; Hicks Pries, C.E.; et al. Beyond clay: Towards an improved set of variables for predicting soil organic matter content. *Biogeochemistry* **2018**, *137*, 297–306. [CrossRef]
56. Kavvadias, V.; Ioannou, Z.; Vavoulidou, E.; Paschalidis, C. Short Term Effects of Chemical Fertilizer, Compost and Zeolite on Yield of Lettuce, Nutrient Composition and Soil Properties. *Agriculture* **2023**, *13*, 1022. [CrossRef]